

# Atmospheric exchanges of CO<sub>2</sub>, CH<sub>4</sub> and N<sub>2</sub>O of temperate forest soils under elevated CO<sub>2</sub> at BIFoR-FACE

Alex Armstrong<sup>1</sup>, Sami Ullah<sup>1</sup>, Liz Hamilton<sup>1</sup>, Elena Vanguelova<sup>2</sup>, Mike Morecroft<sup>3</sup>, Nathan Basiliko<sup>4</sup>, Rob MacKenzie<sup>1</sup>, Niall McNamara<sup>5</sup>  
<sup>1</sup> University of Birmingham, <sup>2</sup> Forest Research, <sup>3</sup> Natural England, <sup>4</sup> Laurentian University, <sup>5</sup> UK Centre for Ecology and Hydrology



## Introduction

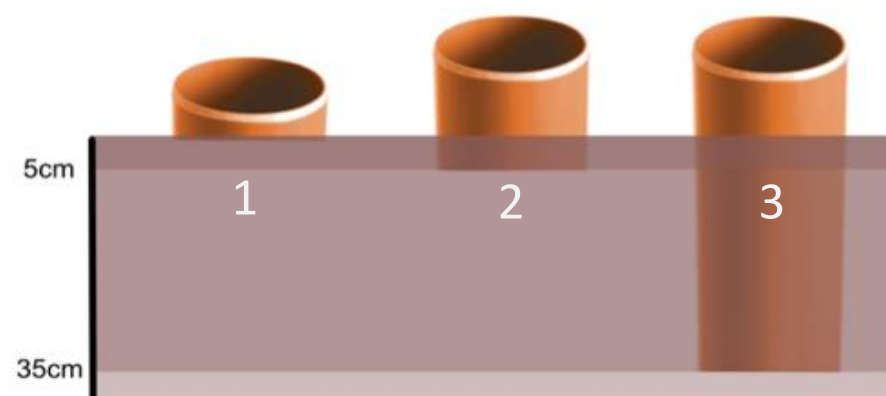
- Atmospheric exchanges of CO<sub>2</sub>, CH<sub>4</sub> and N<sub>2</sub>O of temperate forest soils are an important aspect of the net global warming potential and climate mitigation function of forests.
- However, it's unclear how these fluxes will respond to rising atmospheric CO<sub>2</sub> concentrations (eCO<sub>2</sub>) in temperate forests. Increased carbon sequestration under eCO<sub>2</sub> and storage in biomass and soils can influence the activities of soil microbes responsible for greenhouse-gas (GHG) process dynamics and hence net emissions.
- Initial trends from 2017 - 2020 indicated that eCO<sub>2</sub> arrays had a higher efflux of CO<sub>2</sub> relative to aCO<sub>2</sub> arrays by +20%. However, during 2021 and 2022, eCO<sub>2</sub> arrays have seen a decline in the efflux of CO<sub>2</sub> by -27.5% relative to aCO<sub>2</sub>.
- Sink potential of CH<sub>4</sub> and efflux of N<sub>2</sub>O are also significantly lower under eCO<sub>2</sub> arrays, by -72% and -109% respectively.

## Aims

- Determine inter and intra seasonal patterns in soil gas fluxes under eCO<sub>2</sub> and aCO<sub>2</sub>.
- Partition the relative contribution of autotrophic and heterotrophic fluxes to net emissions.
- Couple with wider available microclimatic and biotic data-streams to assess the key regulatory processes driving flux patterns.

## Methodology

- CO<sub>2</sub> flux rates are determined through long-term LI-8100A continuous gas analyzer system.
- CH<sub>4</sub> & N<sub>2</sub>O are measured through a coupled Picarro G2508 trace gas analyzer.
  - δ<sup>13</sup>C of CO<sub>2</sub> efflux rates measured with loaned Picarro G2201-i (Aug – Nov 2023).
- Automated LI-8200-104 chambers are fitted to 9 collars in each Array, of which there are 3 collar depths.
  - 1 – Shallow collar = Net Emissions.
  - 2 – Medium collar = Net Emissions (minus lateral diffusion).
  - 3 – Deep collar = Pseudo-root exclusion collars.
- Two parallel systems exist, placed within paired eCO<sub>2</sub> and aCO<sub>2</sub> arrays and rotated fortnightly.
  - A1 -> A3
  - A4 -> A2
  - A6 -> A5



## Conclusions

- Efflux of CO<sub>2</sub>, N<sub>2</sub>O and the uptake of CH<sub>4</sub> have declined under eCO<sub>2</sub> during 2022 – 2023 by 40%, 109% and 72% respectively.
- Lower VWC across a soil profile up to 1m was detected in eCO<sub>2</sub> arrays, which should stimulate microbially mediated gas flux process dynamics and increase the efflux of CO<sub>2</sub>, N<sub>2</sub>O and the uptake of CH<sub>4</sub>.
- Higher relative mean differences (Δ%) between pseudo-root exclusion and zero-exclusion chambers coupled with δ<sup>13</sup>C keeling plot R<sup>2</sup> values suggests reduced heterotrophic or enhanced autotrophic contribution to the efflux of CO<sub>2</sub> under eCO<sub>2</sub>.

## Results

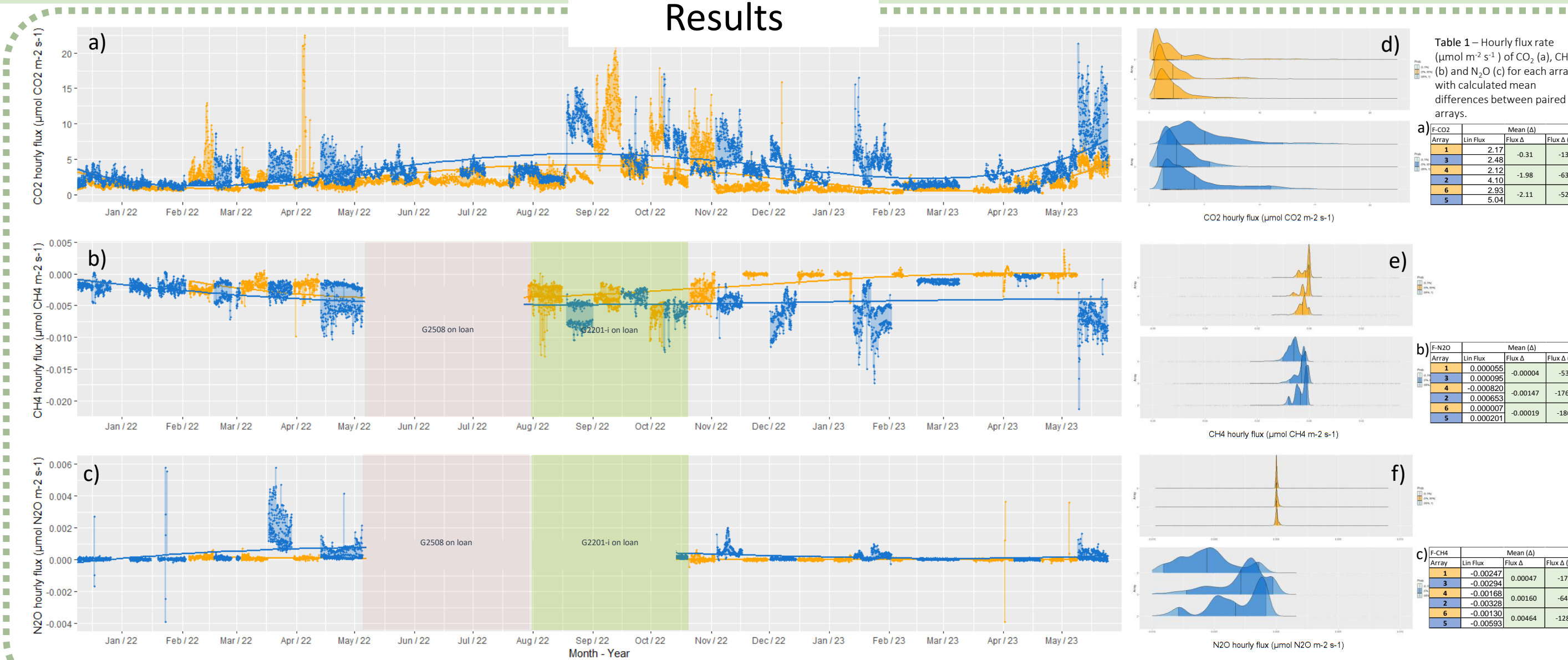


Figure 1 – Hourly flux rate ( $\mu\text{mol m}^{-2} \text{s}^{-1}$ ) of CO<sub>2</sub> (a), CH<sub>4</sub> (b) and N<sub>2</sub>O (c) with corresponding mean values of each gas flux for each array (d, e, f).

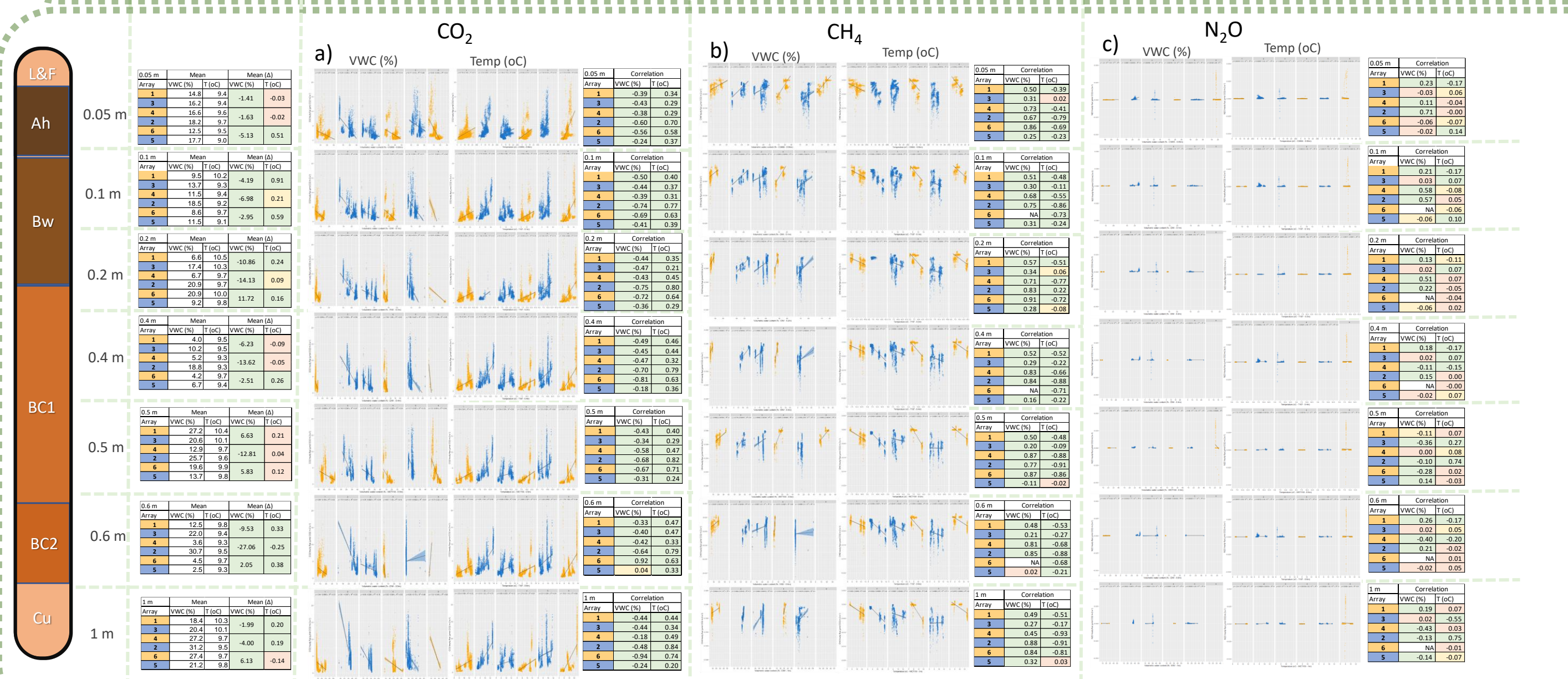


Figure 2 – Hourly flux rate ( $\mu\text{mol m}^{-2} \text{s}^{-1}$ ) of CO<sub>2</sub> (a), CH<sub>4</sub> (b) and N<sub>2</sub>O (c) against volumetric water content (%) and temperature (°C) across 7 soil depths for all Arrays. Corresponding tables contain correlations (Sig 0.01, Sig 0.05, Not Sig).

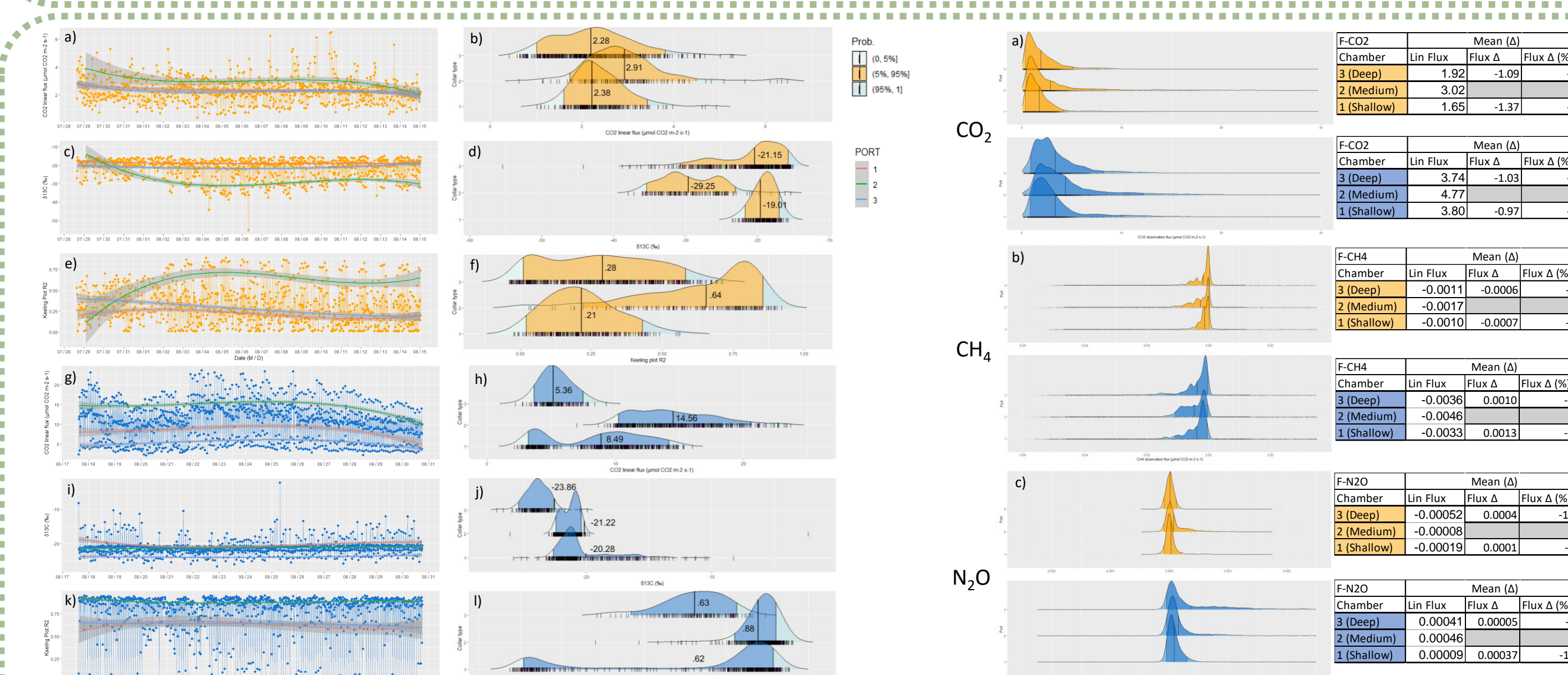


Figure 3 – CO<sub>2</sub> flux rates (a, g) and mean collar values (b, h) with corresponding δ<sup>13</sup>C values derived from linear flux rates (c, d, i, j), with keeling plot derived R<sup>2</sup> values for each observation (e, k) alongside mean R<sup>2</sup> values for each collar type (d, l).

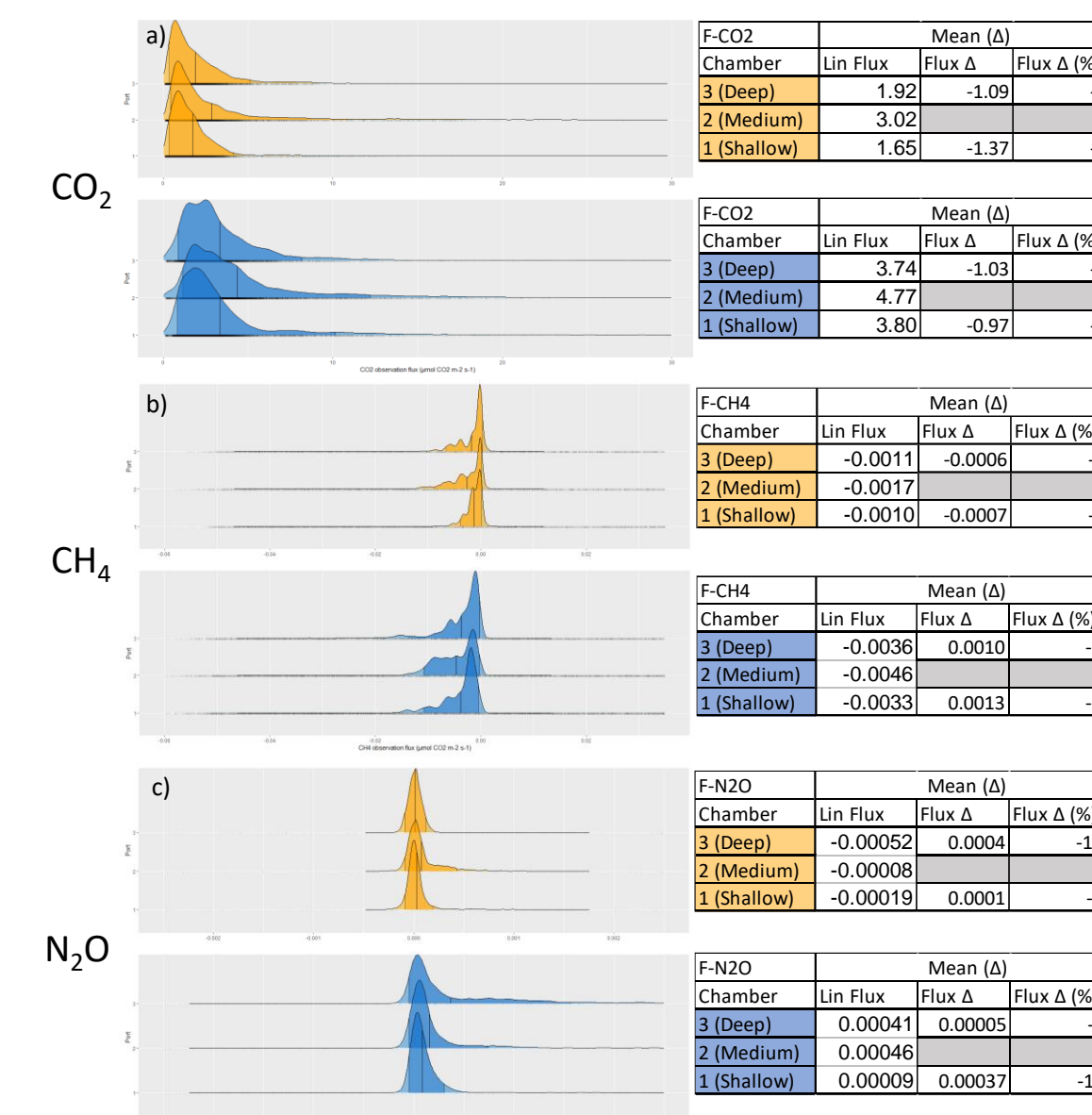


Figure 4 – Mean gas flux rates for CO<sub>2</sub> (a), CH<sub>4</sub> (b) and N<sub>2</sub>O (c) with corresponding tables for mean values and Δ% between shallow, deep and medium collar types.

## Discussion

### Soil gas flux patterns, differences between and within eCO<sub>2</sub> & aCO<sub>2</sub> Arrays.

- Flux of CO<sub>2</sub> is significantly lower under eCO<sub>2</sub> ~-40% (p<.001)\*
  - ~ 1.2  $\mu\text{mol m}^{-2} \text{s}^{-1}$  lower efflux.
  - Stochastic episodes of high efflux in Spring and Autumn.
- Uptake of CH<sub>4</sub> is significantly lower under eCO<sub>2</sub> ~ -72% (p<.001)\*
  - ~ 0.0021  $\mu\text{mol m}^{-2} \text{s}^{-1}$  lower uptake rate.
  - Even under significantly drier soil conditions under eCO<sub>2</sub>.
- Efflux of N<sub>2</sub>O is significantly lower under eCO<sub>2</sub> ~109% (p<.001)\*
  - ~ -0.0000567  $\mu\text{mol m}^{-2} \text{s}^{-1}$  lower efflux.
  - Difference driven by A4, low emissions and episodes of uptake possibly driven by significantly lower soil moisture across all soil depths relative to A2 (-14.3% VWC).

## Discussion

### Soil moisture and temperature; key regulatory drivers of gas fluxes.

- VWC is significantly different between eCO<sub>2</sub> and aCO<sub>2</sub> (p<.001)\*
    - Highly variable across soil profile, equivalent mean difference ~ -4.69%.
      - A1 -> A3 = eCO<sub>2</sub> -4.4%
      - A4 -> A2 = eCO<sub>2</sub> -14.3%
      - A6 -> A5 = eCO<sub>2</sub> +4.6%
  - Temperature shows more homogeneity across both Arrays and depth.
    - A1 -> A3 = eCO<sub>2</sub> +0.17°C
    - A4 -> A2 = eCO<sub>2</sub> +0.03°C
    - A6 -> A5 = eCO<sub>2</sub> +0.27°C
- Strong significantly negative correlation with VWC (eCO<sub>2</sub> = -.44, aCO<sub>2</sub> = -.44) and a strong significantly positive correlation with temperature (eCO<sub>2</sub> = .48, aCO<sub>2</sub> = .48) across all depths and Arrays.  
 Strong significantly positive correlation with VWC (eCO<sub>2</sub> = .67, aCO<sub>2</sub> = .42) and a strong significantly negative correlation with temperature (eCO<sub>2</sub> = -.64, aCO<sub>2</sub> = -.32) across all depths and Arrays.  
 Varied response across both Arrays and depth, showing weak significant correlations with VWC (eCO<sub>2</sub> = .06, aCO<sub>2</sub> = .06), but converse responses to temperature (eCO<sub>2</sub> = -.05, aCO<sub>2</sub> = .09).

## Discussion

### Disseminating gas fluxes and their relative sources; collar type & δ<sup>13</sup>C analysis.

- Higher mean differences (Δ%) between pseudo-root exclusion (3) and zero-exclusion chambers (2) within the eCO<sub>2</sub> arrays suggests a potential decline in the heterotrophic or an increase in the autotrophic contribution to CO<sub>2</sub> effluxes.
  - Coupled with significantly lower δ<sup>13</sup>C keeling plot R<sup>2</sup> values from CO<sub>2</sub> efflux rates, this further suggests a potential shift in source contributions.
  - Potential increased reliance on N-obtaining ectomycorrhizal fungi under eCO<sub>2</sub> driving an enhanced Gadgil effect; effective competitive exclusion of other microbial groups.
- CH<sub>4</sub> & N<sub>2</sub>O shows no significant difference between shallow (1) and pseudo-root exclusion chambers (3) under eCO<sub>2</sub>.
  - Uptake of CH<sub>4</sub> and efflux of N<sub>2</sub>O are significantly lower under eCO<sub>2</sub>, across all Chamber types.